Arabian Journal of Geosciences (2019) 12: 721
https://doi.org/10.1007/s12517-019-4916-9

CAJG 2018: TOPIC 3

Strength estimation of evaporitic rocks using different testing methods

Hasan Arman[1] · Osman Abdelghany[1,2] · Mahmoud Abu Saima[1,2] · Ala Aldahan[1] · Bahaa Mahmoud[1] · Saber Hussein[1] · Abdel-Rahman Fowler[1] · Saaed AlRashdi[3]

Received: 11 May 2019 / Accepted: 30 October 2019 / Published online: 26 November 2019

Abstract

Rock strength is defined as the limit of the ability of a rock to resist stress or deformation without breaking. Testing methods recommended by ISRM (International Society of Rock Mechanics) and ASTM (American Standards Testing Material) include unconfined compressive strength (UCS), point load index (PLI), indirect tensile strength (ITS), Schmidt hammer rebound (SHR), sonic velocity (V_p and V_s), and slake durability index 2nd cycle (I_{d2}). This contribution compares the results of these methods and explores the influence of rock composition and texture on Lower Miocene evaporites from Al Ain city, United Arab Emirates (UAE). These sedimentary rocks are common in the Arabian Peninsula as exposures or in the subsurface where they may constitute the foundations of buildings. A large number of UCS, PLI, ITS, SHR, SV, and I_{d2} tests were carried out on both core samples and rock blocks according to ASTM Standards. Examination of compositional and textural characteristics of representative rock samples was performed using XRD, XRF, polarized-light microscopy, and SEM. The results reveal variable correlations between the rock strength parameters with specific significant values between 0.53 and 0.72. The effect of composition and texture of the evaporitic rocks on their strength behavior is related to impurities such as clay minerals and celestite and grain interlocking textures. Despite the limited compositional variability of the evaporitic rocks (5–10%), the textural variability may present a challenging feature in rock strength testing and should be taken as a primary factor for consideration during applications.

Keywords Rock strength · Evaporitic rocks · Unconfined compressive strength · Point load index · Indirect tensile strength · Slake durability index 2nd cycle

Introduction

Rock strength measurement and characterization of discontinuities (mainly fractures) are important tasks in engineering applications. Overall, rock strength is defined as the limit of the ability of rocks to resist stress or deformation without breaking. In engineering approaches, rock strength may be defined as the inherent strength of an isotropic rock under wet or dry conditions. Nevertheless, rock masses are anisotropic and therefore, the strength of rocks is influenced by the presence of impurities, zones of weakness, and/or discontinuities (Hawkins 1998).

Rapid changes of rock structure on the meter scale (i.e., presence of layering, fractures, faults, folds), rock texture (grain size, cementation, dissolution), and even mineralogy (percentage of clay minerals, sulfates, etc., and presence of water) have always created problems in generalizing overall bulk mechanical and physical properties, such as rock strength, porosity, etc. Thus, true homogeneity may only exist at a small scale, perhaps a few cubic decimeters, leading to problems for engineers when they are forced to deal with much larger scales of rock masses. Inhomogeneity and rapid changes in the physical properties of rock masses commonly cause unexpected rock failure, particularly when these factors

This paper was selected from the 1st Conference of the Arabian Journal of Geosciences (CAJG), Tunisia 2018

Responsible Editor: Amjad Kallel

✉ Hasan Arman
harman@uaeu.ac.ae

[1] College of Science, Geology Department, United Arab Emirates University, P.O. Box: 15551, Al Ain, UAE

[2] Faculty of Science, Geology Department, Ain Shams University, Cairo 11566, Egypt

[3] University of the Western Cape, P/Bag X17, Cape Town 7535, South Africa

are combined with the presence of water. All these factors underline the importance of measuring the rock strength via in situ or laboratory methods (Marinos and Hoek 2001; Erguler and Ulusay 2009; Yilmaz 2010; Arman et al. 2013a, b, 2014, 2017).

However, measurement of rock strength in either in situ or laboratory environments is relatively expensive, time-consuming, and requires considerable efforts in rock sampling, preparation, and laboratory tests. Quite a large number of specimens must be tested in order to produce a representative value for a large rock exposure. Therefore, it is common to measure rock strength using several testing methods and approaches (Arman et al. 2013a, b, 2014, 2017). A number of methods have been recommended for the testing of rock strength. Among these are the unconfined compressive strength (UCS), indirect tensile strength (ITS), point load index (PLI), Schmidt hammer rebound (SHR), sonic velocity (V_p and V_s), and slake durability index 2nd cycle (I_{d2}).

There are few available studies concerning strength estimations of evaporitic rocks. Yilmaz and Sendir (2002) performed correlation of SHR with UCS and Young's modulus (E) in gypsum. Their study concluded that it may be possible to estimate UCS and E of gypsum from the SHR number using their proposed empirical equations. They also suggested that their equations must be used only for gypsum to give an acceptable accuracy in the preliminary stage of designing structures. Yilmaz and Yuksek (2008, 2009) thought that it may possible to predict UCS and even E of gypsum using artificial intelligence-based techniques such as fuzzy interface system (FIS), multiple regression (MR), genetic programing (GP), artificial neural network (ANN), and adaptive neuro-fuzzy inference system (ANFIS) models. However, these findings should be treated with caution due to the limited number of data analyses. Heidari et al. (2012) studied the relationships between UCS, ITS, and PLI (air-dried and saturated and three methods of axial, diametrical, and irregular) for gypsum rock samples and developed appropriate empirical equations. Thus, they demonstrated the possibility of estimating UCS and ITS using fast, practical, and economical PLI tests. However, they also advised that their empirical equations be used for the local gypsum rocks, excluding those of other regions. Salah et al. (2014) carried out laboratory studies on crystalline gypsum in order to develop a dataset for predicting the UCS of rock specimens from PLI tests. They found the data to be highly scattered, and they provided empirical equations for use as conservative design values.

This paper presents comprehensive laboratory mechanical investigations of the evaporitic rocks at selected United Arab Emirates (UAE) sites, with the aim of providing data that can be used to better constrain rock strength properties. The highly variable composition and texture of the evaporites results in their vulnerability to in situ chemical and mechanical changes due to changes in groundwater chemistry and climatic conditions, which can influence the durability of evaporites over time. The present work aims to provide vital data and guidelines that will help reduce the cost of hazards assessment for the engineering projects sited on evaporite rocks.

Geological setting, sampling, and analytical techniques

Evaporitic rocks of the Lower Fars (Gachsaran) Formation of Early Miocene age (23–16 Myr) exist as 300 m outcrops and at different depths below land surface in Al Ain city of the UAE (Abdelghany et al. 2015). The Jabal Hafit mountain south of Al Ain city, UAE, exposes a lower tertiary to Miocene limestone, marl, and evaporite sequence exceeding 1200 m in thickness (Boukhary et al. 2002) (Fig. 1). Beneath the Gachsaran Formation evaporites are dominantly carbonate rocks. The Miocene evaporite beds were deposited conformably on the top of the Lower Oligocene Asmari Formation on the eastern limb of the Jabal Hafit Anticline (Styles et al. 2006; Thomas et al. 2014).

The Lower Miocene evaporitic rocks consist mainly of gypsiferous layers and veins that are interbedded with friable marls and mudstones of 3 to 5 m thickness. The gypsiferous layers are composed of a variety of nodular, coarsely crystalline, and finely granular gypsum and are well exposed in a quarry east of Jabal Hafit (Fig. 1). Forty-eight-representative evaporite rock block samples were collected over a stratigraphic interval of about 20 m to be used in this investigation. To reduce effects of anisotropy, thinly bedded (< 1 cm thick) rocks were avoided.

The compositional and textural characteristics of the evaporite samples were determined using polarized light microscopy, scanning electron microscopy (SEM), X-ray diffraction (XRD), and X-ray fluorescence (XRF). A total of 213 core samples (NX, 54 mm in diameter) were obtained from the 48 evaporite blocks. A large number of tests including 114 UCS, 115 PLI, 124 ITS, and 231 SV (for V_p and V_s) were performed according to ASTM Standards (ASTM 2008a). In addition, from each block, a representative slake durability index (SDI) test sample was prepared according to ASTM (2016a) procedure. The UCS, PLI, ITS, SV, and SDI tests were carried out following ASTM standards (ASTM 1995, 2008b, c, 2016a, b).

Results

Composition and texture of the rocks

Material investigation of the evaporites revealed three major textural and compositional groups (Fig. 2). The first group (G1)

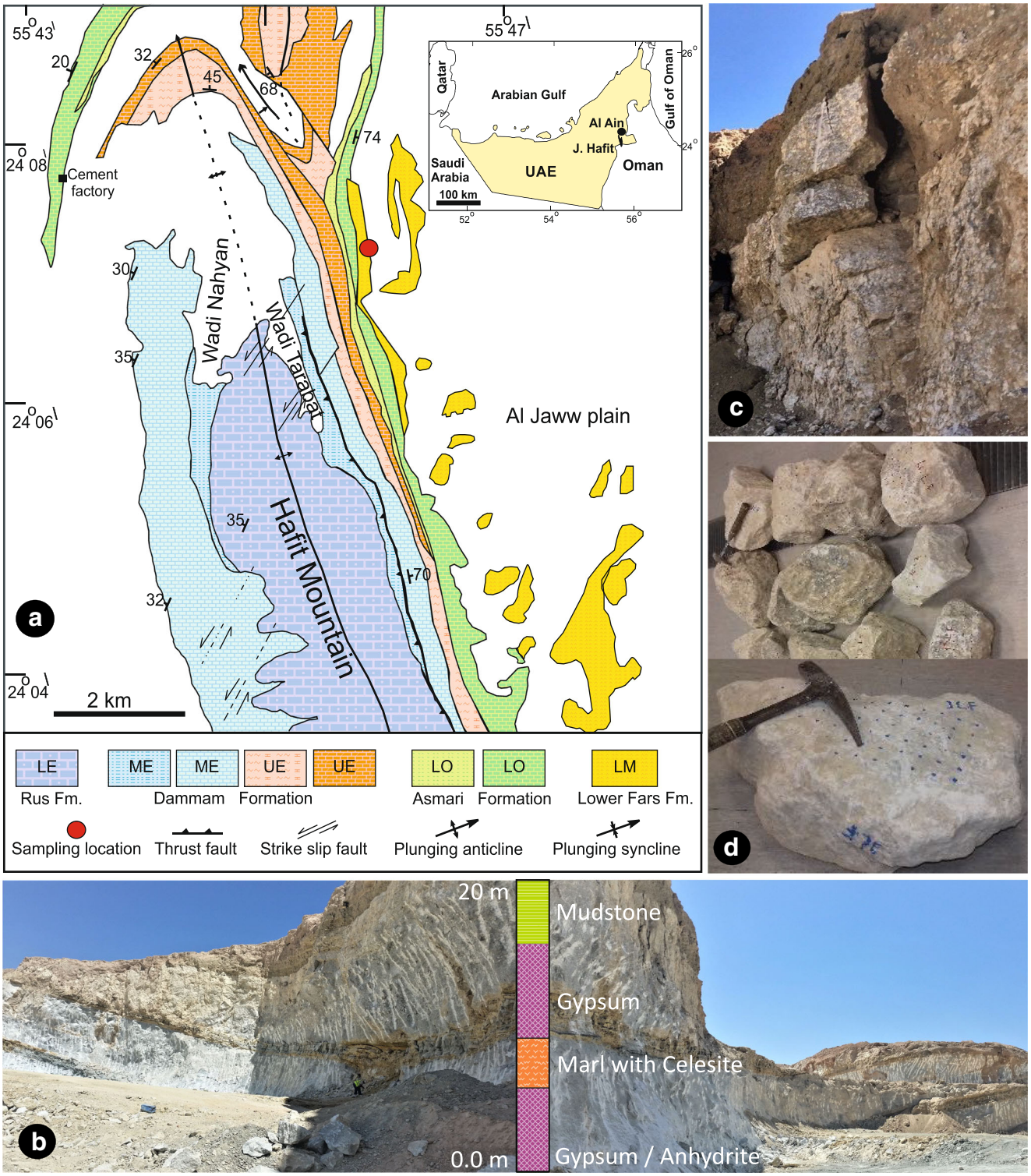

Fig. 1 **A** Geological map and sampling location with exposure and rock block samples. LE Lower Eocene, M–UE Middle to Upper Eocene, LO Lower Oligocene and LM Lower Miocene **B** and **C** Photographs of quarry sample site with measured stratigraphic section **D** Boulder-sized rock samples showing pattern of test points for SHR

includes samples E3, E4, and E23 and shows dominance of platy-like, radiating, and partly aggregated crystals of gypsum that vary from coarse (> 1 mm) to finer grainsizes (Fig. 2). The texture is interlocking with sparse porosity and presence of matrix of muddy aggregates (clay minerals, quartz, and feldspars). There are some zones of dolomitic texture; however, neither the

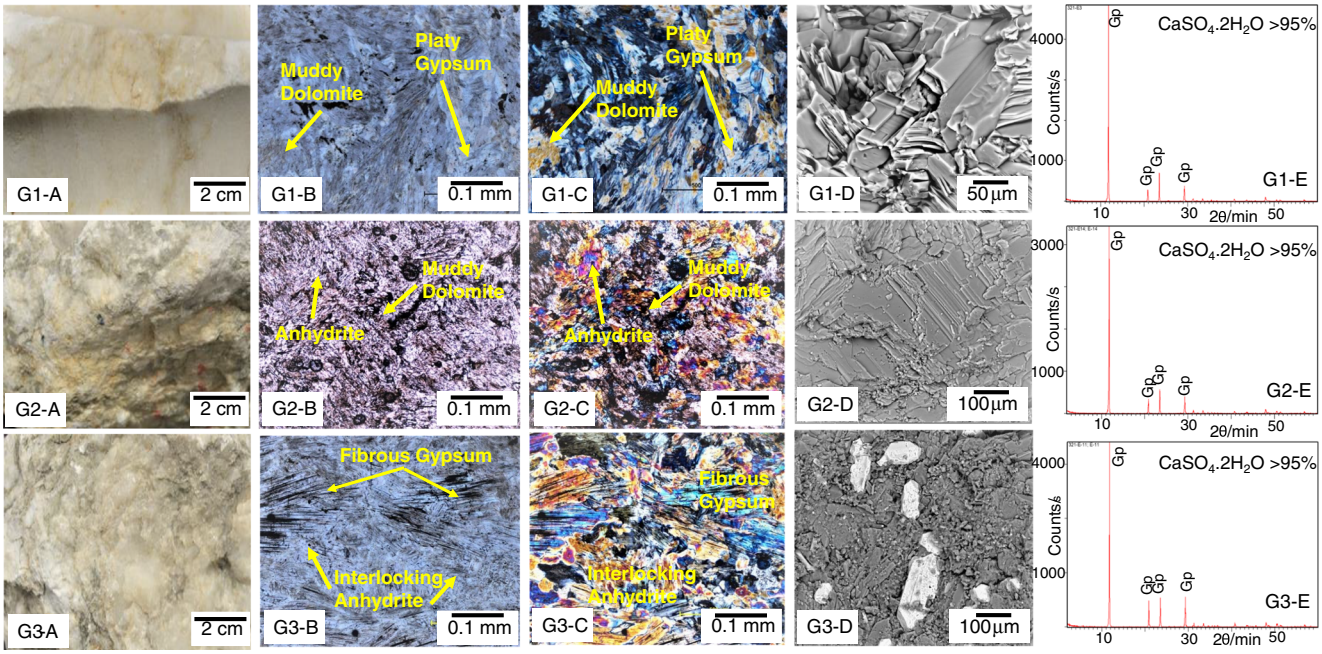

Fig. 2. G1 Sample of 1st group, A. Rock sample, B–C. Thin-section images under plane and cross-polarized light showing coarse (>1 mm) radiated platy gypsum, D. SEM image showing interlocked gypsum crystals, E. XRD showing the major mineral > 95% gypsum and the remaining is matrix and dolomite; G2 Sample of 2nd group, A. Rock sample, B–C. Thin-section images under plane and cross-polarized light showing gypsum with relics of anhydrite and dolomite, D. SEM image showing prismatic gypsum crystals, E. XRD showing the major mineral > 95% gypsum and minor <5% matrix and dolomite; G3 Sample of 3rd group, A. Rock sample, B–C. Thin-section images under plane and cross-polarized light showing acicular (needle-like) and fibrous gypsum crystals, D. SEM image micro-rhombi-prismatic crystals (< 10 micron in size) occur in these samples suggesting a mixture of dolomite and anhydrite, E. XRD showing the major mineral > 95% gypsum and both the matrix and dolomite content of <5%

matrix nor dolomite was evident on the XRD scans suggesting concentrations of < 5%. In addition to the microscopic observation, the presence of dolomite and clay minerals was confirmed by the chemical data and correlation between the chemical components (Table 1). Calculation of the mineralogical formula indicates that the analyzed evaporites contain > 90% gypsum with the remainder represented by matrix and dolomite.

The evaporite rocks of the second group (G2) include representative samples E11 and E20 and are composed primarily of granular aggregates and crystalline gypsum with grain long-axis-preferred orientation. The texture of the samples of massive and lacking in the abundant microporosity is observed in G1 samples. The content of matrix material appears more abundant than in G1 as shown by the microscopic

Table 1 Chemical composition of representative evaporite samples (*L.O.I* loss on ignition)

wt. %	Group 1			Group 2		Group 3			
	E3	E4	E23	E11	E20	E13	E14	E17	E26
SiO_2	0.23	0.37	< 0.01	1.19	0.60	0.45	0.26	0.49	0.34
TiO_2	0.01	0.01	0.01	0.01	0.01	0.01	0.01	0.01	0.01
Al_2O_3	0.11	0.15	< 0.01	0.36	0.19	0.16	0.10	0.11	0.19
Fe_2O_3	0.12	0.12	0.07	0.23	0.18	0.12	0.12	0.13	0.13
MnO	0.01	0.01	0.01	0.01	0.01	0.01	0.01	0.01	0.01
MgO	0.29	0.24	0.13	0.93	0.80	0.41	0.38	0.40	0.51
CaO	33.45	33.30	33.55	32.90	34.30	33.38	33.27	34.95	33.19
Na_2O	< 0.01	< 0.01	< 0.01	< 0.01	< 0.01	< 0.01	< 0.01	< 0.01	< 0.01
K_2O	0.01	0.02	< 0.01	0.07	0.04	0.03	0.01	0.03	0.01
Cl	0.07	0.06	0.05	0.08	0.06	0.07	0.06	0.09	0.10
SO_3	44.95	45.10	45.75	42.44	43.26	45.10	44.60	40.58	44.60
L.O.I	20.37	20.30	20.10	21.39	20.20	19.90	20.80	22.86	20.56

Table 2 The statistical results for the tested samples

	UCS (MPa)	PLI (MPa)	ITS (MPa)	SHV (N) blocks	SV (km/s)		SDI (%)
					V_p	V_s	I_{d2}
Number of samples	114	115	124	48	231	231	48
Minimum	15.55	0.53	1.47	18	4.19	1.65	8.42
Maximum	40.03	2.19	4.39	28	6.15	3.43	60.77
Average	24.57	1.39	2.80	24	5.41	2.52	36.21
Standard deviation	4.99	0.42	0.67	3	0.41	0.35	14.82

examination (Fig. 2) and chemical data (Table 1), with higher SiO_2, MgO, Al_2O_3, and Fe_2O_3. The matrix mineralogy is not evident in the XRD diagram, suggesting < 5% matrix, confirmed by the mineralogical formula calculation.

The third group (G3) of evaporite rocks includes representative samples E13, E14, E17, and E26 and is dominated by gypsum showing platy to acicular and fibrous crystals (Fig. 2). Microscopic rhombic crystals (< 10 micron in size) are found in these samples pointing to a mixture of dolomite and anhydrite (Fig. 2). However, as with the previous samples, these minor minerals are not evident in the XRD diagram. The matrix content in this group of evaporites is intermediate between those of G1 and G2.

It is important to mention that the chemical analyses show sodium and potassium salts to be uncommon in all the groups of evaporite rocks described above. Traces of celestite ($SrSO_4$) crystals occur in all samples based on the chemical data and SEM examination. In most of the samples, relics of anhydrite were also observed (Fig. 2).

Rock strength

The number of samples and rock strength average values are shown in Table 2. Based on the obtained results, the UCS values for the samples ranged between 15.55 and 40.03 MPa, with an average of 24.57 MPa, while the average values of PLI and ITS were 1.39 and 2.8 MPa. PLI values varied from 0.53 to 2.19 MPa, and ITS ranged from 1.47 and 4.39 MPa. As shown in Table 2, the average value of SHV on rock blocks was 24 (N) and the minimum and maximum values were 18 and 28 (N), respectively. The minimum and maximum values of V_p and V_s were 4.19–6.15 and 1.65–3.43 km/s, respectively, with an average of 5.41 and 2.52 km/s. The SDI values of samples varied between 8.42 and 60.77 (%) with an average of 36.42 (%).

The Pearson linear correlation coefficients obtained from plotting chemical data against rock strength indices for the representative samples are shown in Table 3. The correlation R values show significant positive coefficients between SiO_2, Fe_2O_3, Al_2O_3, MgO, and K_2O that are common constituents of the matrix (clay minerals). The negative correlation with sulfate (SO_3) against other chemical and strength parameters is insignificant for all components apart from CaO (−0.63) indicating the connection to gypsum. The estimated correlation between the chemical components and rock strength data suggest fluctuating relationships and correlation coefficients < 0.6 for all the components. These correlations and effects of textural variability of the rocks are further discussed in the next section.

Table 3 Correlation coefficient (R-value) matrix between the chemical components and rock strength data

wt. %	SiO_2	Al_2O_3	Fe_2O_3	MgO	CaO	K_2O	Cl	SO_3
Al_2O_3	0.94							
Fe_2O_3	0.96	0.93						
MgO	0.89	0.88	0.96					
CaO	− 0.10	− 0.33	− 0.09	− 0.04				
K_2O	0.98	0.87	0.92	0.86	0.00			
Cl	0.36	0.44	0.32	0.34	0.10	0,24		
SO_3	− 0.61	− 0.40	− 0.57	− 0.54	− 0.63	− 0,62	− 0,52	
L.O.I	0.37	0.17	0.28	0.21	0.53	0.34	0.56	− 0.90
UCS (MPa)	0.24	0.24	0.38	0.48	0.56	0.29	0.18	− 0.43
ITS (MPa)	0.48	0.36	0.53	0.30	0.15	0.50	− 0.17	− 0.41
PLI ($I_{s(50)}$) (MPa)	0.34	0.49	0.40	0.33	− 0.29	0.33	− 0.14	0.20
V_p (km/s)	0.43	0.54	0.46	0.48	0.01	0.38	0.59	− 0.31
I_{d2} (%)	0.43	0.53	0.42	0.26	− 0.17	0.40	0.24	− 0.15

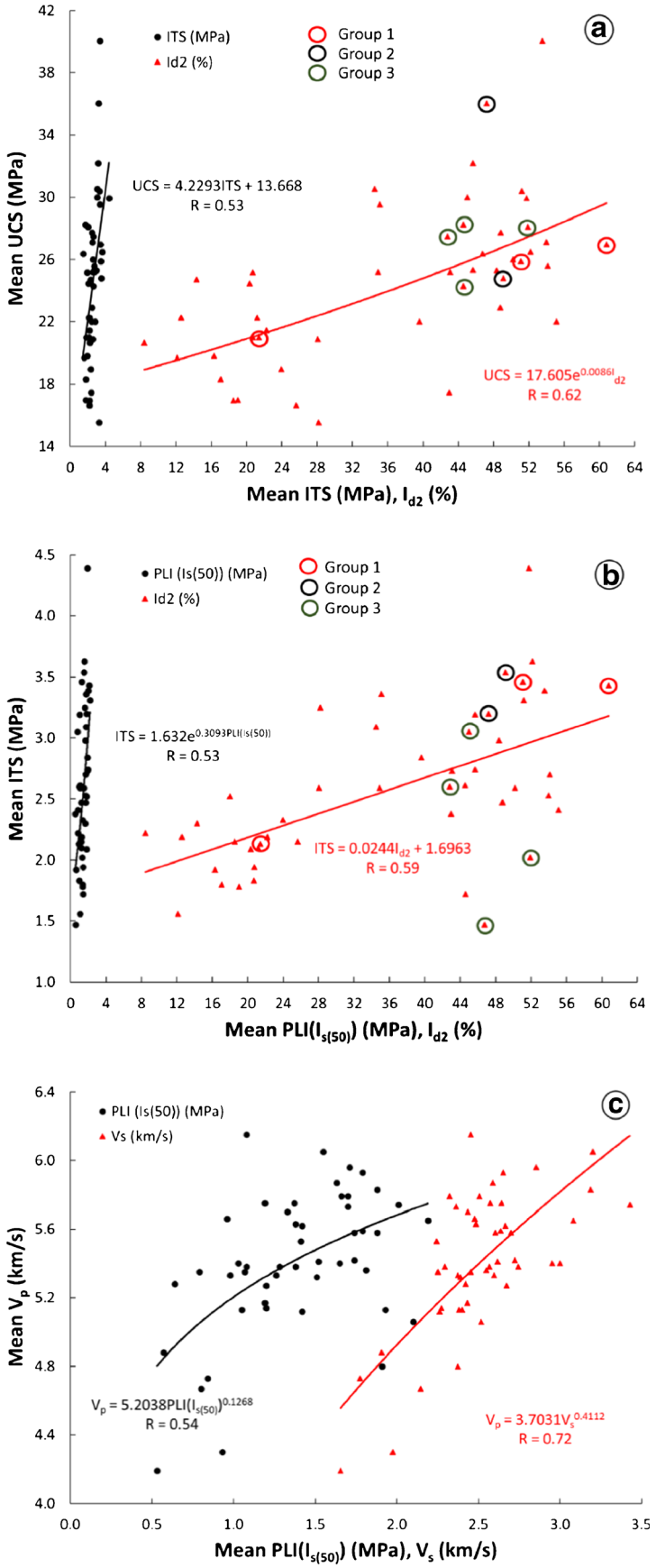

Fig. 3 **a** Mean ITS and I_{d2} versus mean UCS, **b** Mean PLI ($I_{s(50)}$) and I_{d2} versus ITS, **c** Mean PLI($I_{s(50)}$) and V_s versus mean V_p

Discussion

According to the intact rock classification (Marinos and Hoek 2001), the studied evaporite rocks can be classified as either medium strong or weak using the UCS and PLI mean values, respectively. In order to establish the empirical relations between dependent and independent variables, simple regression analyses were carried out. The equation of the line of best fit and the correlation coefficient (R) were estimated for selected pairs of strength criteria, plotted one against the other (Fig. 3a–c). In Fig. 3a, the relations between UCS on the one hand, and ITS and I_{d2} on the other, are approximated by linear (UTS versus ITS) and exponential equations (UTS versus I_{d2}) with R values 0.53 and 0.62, respectively. Similarly, linear and exponential equations with R values 0.53 and 0.59 represent the statistically best representation of the relations of ITS plotted against PLI ($I_{s(50)}$) and I_{d2} (Fig. 3b). In addition, the best-fit correlation lines for V_p data plotted against PLI ($I_{s(50)}$) and V_s data are characterized by power equations with R values of 0.54 and 0.72, respectively. Overall, the relations between UTS plotted against ITS and I_{d2} (Fig. 3a); ITS plotted against PLI ($I_{s(50)}$) and I_{d2} (Fig. 3b); and V_p plotted against PLI ($I_{s(50)}$) and V_s (Fig. 3c) are associated with moderate to medium values of correlation coefficients.

Published data (Yilmaz and Sendir 2002; Yilmaz and Yuksek 2008, 2009; Heidari et al. 2012; Salah et al. 2014)

Table 4 Previous studies and the present study on the correlations between *UCS*, *E*, *PLI* ($I_{s(50)}$), V_p, V_s, *ITS*, *and* I_{d2}, for evaporitic rocks

Researchers	Equations	R	Rock type
Yilmaz and Sendir 2002	$E = e(1.146 + 0.054SHV)$	0.95	Gypsum
	$UCS = e(0.818 + 0.059SHV$	0.98	
Yilmaz and Yuksek 2008	$UCS = 2.14PLI(I_{s(50)}) - 9.0859$	0.90	Gypsum
	$E = 10.943PLI(I_{s(50)}) + 0.8527$	0.75	
Yilmaz and Yuksek 2009	$UCS = 10.52PLI(I_{s(50)}) - 3.966$	0.75	Gypsum
	$UCS = -28.429Ln(n) + 78.989$	− 0.89	
	$UCS = -10.163Ln(WA) + 30.577$	− 0.91	
	$UCS = 4.011e^{0.038SHV}$	0.88	
	$UCS = 3.9348e^{0.6129Vp}$	0.91	
	$E = -39.1Ln(n) + 110.31$	− 0.91	
	$E = -13.94Ln(WA) + 43.712$	− 0.92	
	$E = 14.122PLI(I_{s(50)}) - 2.745$	0.75	
	$E = 6.9986e^{0.0345SHV}$	0.89	
	$E = 6.8545e^{0.5561Vp}$	0.91	
Heidari et al. 2012	$UCS = 10.99PLI(I_{s(50)}) + 7.04$ *(axial)*	0.96	Gypsum (*air dry samples*)
	$UCS = 11.96PLI(I_{s(50)}) + 10.64$ *(diametric)*	0.97	
	$UCS = 13.29PLI(I_{s(50)}) + 5.25$ *(irregular)*	0.95	
	$UCS = 5.58PLI(I_{s(50)}) + 21.92$ *(axial)*	0.96	*(Saturated samples)*
	$UCS = 7.56\ PLI(I_{s(50)}) + 23.68$ *(diametric)*	0.97	
	$UCS = 3.49PLI(I_{s(50)}) + 24.84$ *(irregular)*	0.94	
	$ITS = 1.36PLI(I_{s(50)}) + 2.06$ *(axial)*	0.96	(*Air dry samples*)
	$ITS = 1.77PLI(I_{s(50)}) + 2.57$ *(diametric)*	0.93	
	$ITS = 0.88PLI(I_{s(50)}) + 2.7$ *(irregular)*	0.98	
	$ITS = 2.88PLI(I_{s(50)}) - 0.07$ *(axial)*	0.94	*(Saturated samples)*
	$ITS = 2.9\ PLI(I_{s(50)}) + 1.1$ *(diametric)*	0.88	
	$ITS = 3.47PLI(I_{s(50)}) - 0.52$ *(irregular)*	0.93	
Salah et al. 2014	$UCS = 11.08PLI(I_{s(50)})$ *(crystalline*	0.83	Gypsum
	$UCS = 11.24PLI(I_{s(50)})$ *(weak crystalline)*	0.74	
This study 2019	$UCS = 4.2293ITS + 13.668$	0.53	Evaporites
	$UCS = 17.792e^{0.0083I_{d2}}$	0.62	
	$ITS = 1.632e^{0.3093PLI\ (Is(50))}$	0.53	
	$ITS = 0.0244I_{d2} + 1.6963$	0.59	
	$V_p = 5.2038PLI(I_{s(50)})^{0.1268}$	0.54	
	$V_p = 3.7031V_s^{0.4112}$	0.72	

UCS uniaxial compressive strength (MPa), *E* modulus of elasticity (GPa), *SHV* Schmidt rebound value (N), *PLI* ($I_{s(50)}$) point load index value (for 50 mm in diameter size sample) (MPa), V_p P wave velocity (km/s), V_s S wave velocity (km/s), *ITS* indirect tensile strength (MPa), *WA* water absorption (%), *n* = Porosity (%), I_{d2} slake durability index 2nd cycle (I), *R* regression coefficient

have quantified the relations between rock strength indices (UCS, PLI, E, etc.) and physical properties (n and WA) of gypsum, using a variety of equations to analyze the data (Table 4). The results revealed relationships ranging between positive and negative trends with correlation coefficients (R) for gypsum that are higher (0.74–0.98) than ours (0.53–0.72). However, all published data shown in Table 4 clearly indicate that the provided empirical equations should not be viewed as applicable for all gypsum, even where R values are high (Yilmaz and Sendir 2002; Yilmaz and Yuksek 2008, 2009; Heidari et al. 2012; Salah et al. 2014). The contrast in the R-values between published data and our data may relate to the compositional and textural changes that were correlated to the rock strength data in other works.

The impact of compositional variability (mineralogical and chemical) of the evaporite rocks on the rock strength values is not highly significant as shown by the correlation coefficient data (Table 3). Occurrence of impurities such as clay minerals seem to positively correlate with UCS (MPa), ITS (MPa), PLI ($I_{s(50)}$) (MPa),V_p (km/s), and I_{d2} (%) as indicated by the relatively moderate R values. These correlations are also apparent with plotting of the different groups in the rock strength correlation in Fig. 3a–b, especially in the SDI values. Despite this apparently limited compositional control on the rock strength properties of the rocks, the textural variability may be a significant factor as shown by the rather variable textures of the rocks (Fig. 2). The textural difference, crystal size and shapes, porosity (intra- and intercrystalline) and compaction effect, introduces variations in the mechanical properties of the rocks. Therefore, the mean values and relationships between the tests are unequivocally affected by the compositional and textural changes in the rocks, though simple and direct relationships are difficult to find. This is because in addition to the microscopic textural variability, there are also macro changes (on mm and cm scales) that include aggregation, thin lamination, and occurrence of interlayering of marl and mudstones that further complicate the behavior of strength properties of the rocks.

The rock strength values of the evaporite rocks tested here are also lower than those for carbonate rocks in the same area (Arman et al. 2013a, b, 2014). This is another important issue for the evaluation of rock strength properties in the area. In most cases, the evaporite rocks are interlayered or mixed with carbonate rocks in the subsurface, and estimating the strength properties for both lithologies provides a complimentary data set for engineering evaluation of this terrain.

Conclusions

Following standard rock strength testing methods for evaporite rocks of the Al Ain area, UAE, the results indicate variable correlations between the rock strength parameters. These variations are related to effects of composition and texture of the evaporite rocks, including occurrence of impurities, such as clay minerals and celestite, and the development of crystalline interlocking textures. Despite the limited compositional variability of the evaporitic rocks (5–10%), the textural variability may represent a challenging feature in rock strength testing and should be taken as a primary factor for consideration during applications. The data also suggest that further caution should be taken during engineering applications dealing with evaporate rocks, due to the sensitivity of their strength properties to textural variations.

Acknowledgments This research was funded by the United Arab Emirates University, Research Affairs with the research project number UPAR 2016 – 31S252. The authors wish to express special thanks to the research assistant, technicians and students who participated in the field and laboratory work.

References

Abdelghany O, Abu Saima M, Arman H, Fowler A (2015) Gypsiferous bedrocks and soils of Abu Dhabi and their implications for engineering geozoning, In Proceedings of the Third International Conference on Engineering Geophysics-Leading through Creativity, Innovation and Sustainability. Al Ain, United Arab Emirates, November 15-18, EG26, 156-159.

Arman H, Hashem W, Abdelghany O, Aldahan A (2013a) On the accuracy of the in-situ Schmidt hammer tests on carbonate rocks. In Proceedings of Eurock 2013-Rock Mechanics for Resources, Energy and Environment-The 2013 ISRM International Symposium. Wraclow, Poland, 23-26 September, 189-193.

Arman H, Hashem W, Abdelghany O, Aldahan A (2013b) Evaluation of laboratory Schmidt hammer tests on carbonate rocks. In Proceedings of the Second International Conference on Engineering Geophysics, Al Ain, United Arab Emirates, 24-27 November, EG37, 234-237.

Arman H, Hashem W, Tokhi EM, Abdelghany O, Saiy EA (2014) Petrographical and geomechanical properties of the Lower Oligocene limestones from Al Ain city, United Arab Emirates. Arab J Sci Eng 39(1):261–271

Arman H, Hashem W, Abdelghany O, Aldahan A (2017) Effects of lithofacies and environment on in situ and laboratory Schmidt hammer tests: a case study of carbonate rocks. Q J Eng Geol Hydrogeol 50:179–186

ASTM D2845-08 (2008a) Standard test method for laboratory determination of pulse velocities and ultrasonic elastic constants of rock (Withdrawn 2017). ASTM International, West Conshohocken.

ASTM D2936-08 (2008b) Standard test method for direct tensile strength of intact rock core specimens (Withdrawn 2017). ASTM International, West Conshohocken.

ASTM D2938-95 (1995) Standard test method for unconfined compressive strength of intact rock core specimens. ASTM International, West Conshohocken.

ASTM D4543-08e1 (2008c) Standard practices for preparing rock core as cylindrical test specimens and verifying conformance to dimensional and shape tolerances (Withdrawn 2017). ASTM International, West Conshohocken.

ASTM D4644-16 (2016a) Standard test method for slake durability of shales and other similar weak rocks. ASTM International, West Conshohocken.

ASTM D5731-16 (2016b) Standard test method for determination of the point load strength index of rock and application to rock strength classifications. ASTM International, West Conshohocken.

Boukhary M, Abdelghany O, Bahr S (2002) Nummulites alsharhani n.sp. (Late Lutetian) from Jabal Hafit and Al Faiyah: western side of the Northern Oman Mountains, United Arab Emirates. Revue Paleobiol Geneve 21:575–585

Erguler ZA, Ulusay R (2009) Water-induced variations in mechanical properties of clay-bearing rocks. Int J Rock Mech Min 46:355–370

Hawkins AB (1998) Aspects of rock strength. Bull Eng Geol Environ 57: 17–30

Heidari M, Khanlari GR, Kaveh MT, Kargarian S (2012) Predicting the uniaxial compressive and tensile strengths of gypsum rock by point load testing. Int J Rock Mech Min 45(2):256–273

Marinos P, Hoek E (2001) Estimating the geotechnical properties of heterogeneous rock masses such as Flysch. Bull Eng Geol Environ 60: 85–92

Salah H, Omar M, Shanableh A (2014) Estimating unconfined compressive strength of sedimentary rocks in United Arab Emirates from point load strength index. J Appl Math Phy 2:296–303

Styles MT, Ellison RA, Arkley SLB, Crowley Q, Farrant AR, Goodenough KM, Mckervey JA, Pharaoh TC, Phillips ER, Schofield D, Thomas RJ (2006) The geology and geophysics of the United Arab Emirates. In: Geology, vol 2. Ministry of Energy, United Arab Emirates

Thomas RJ, Ellison RA, Farrant AR, Goodenough KM, Kimbell GS, Newell AJ, Pharaoh TC, Phillips ER, Styles MT (2014) Geologic evolution of the United Arab Emirates-over six hundred million years of Earth history. Ministry of Energy, United Arab Emirates

Yilmaz I (2010) Influence of water content on the strength and deformability of gypsum. Int J Rock Mech Min 47:342–347

Yilmaz I, Sendir H (2002) Correlation of Schmidt hardness with unconfined compressive strength and Young's modulus in gypsum from Sivas (Turkey). Eng Geol 66(3):211–219

Yilmaz I, Yuksek AG (2008) An example of artificial neural network (ANN) application for indirect estimation of rock parameters. Int J Rock Mech Min 41(5):781–795

Yilmaz I, Yuksek AG (2009) Prediction of the strength and elasticity modulus of gypsum using multiple regression, ANN and ANFIS models. Int J Rock Mech Min 46(4):803–810